



Contents lists available at ScienceDirect

Bioorganic & Medicinal Chemistry Letters

journal homepage: www.elsevier.com/locate/bmcl

Design and synthesis of novel 2-(indol-5-yl)thiazole derivatives as xanthine oxidase inhibitors

Jeong Uk Song^{a,b}, Sung Pil Choi^b, Tae Hun Kim^b, Cheol-Kyu Jung^b, Joo-Youn Lee^b, Sang-Hun Jung^{a,*}, Geun Tae Kim^{b,*}

^a College of Pharmacy, Chungnam National University, Daejeon 305-764, Republic of Korea

^b Research & Development, LG Life Sciences Ltd, 188 Munji-ro, Yuseong-gu, Daejeon 305-380, Republic of Korea

ARTICLE INFO

Article history:

Received 6 July 2014

Revised 11 January 2015

Accepted 22 January 2015

Available online xxx

Keywords:

Gout

Hyperuricemia

Xanthine oxidase inhibitors

2-(Indol-5-yl)thiazole

ABSTRACT

Xanthine oxidase (XO) inhibitors have been widely used for the treatment of gout. Indole rings are frequently used as active scaffold in designing inhibitors for enzymes. Herein, we describe the structure–activity relationship for novel xanthine oxidase inhibitors based on indole scaffold. A series of novel tri-substituted 2-(indol-5-yl)thiazole derivatives were synthesized, and their *in vitro* inhibitory activities against xanthine oxidase and *in vivo* efficacy lowering uric acid level in blood were measured. Among them, 2-(3-cyano-2-isopropylindol-5-yl)-4-methylthiazole-5-carboxylic acid exhibits the most potent XO inhibitory activity (IC_{50} value: 3.5 nM) and the excellent plasma uric acid lowering activity. Study of structure activity relationship indicated that hydrophobic moiety (e.g., isopropyl) at 1-position and electron withdrawing group (e.g., CN) at 3-position of indole ring and small hydrophobic group (CH_3) at 4-position of the thiazole ring enhanced the XO inhibitory activity. Hydrophobic substitution such as isopropyl at 1-position of the indole moiety without any substitution at 2-position has an essential role for enhancing bioavailability and therefore for high *in vivo* efficacy.

© 2015 Elsevier Ltd. All rights reserved.

Gout is commonly recognized as recurrent pains of acute inflammatory arthritis. High level of uric acid in blood, or hyperuricemia causes such symptoms by inducing the precipitation of monosodium urate crystals.¹ The disease occurs by overproduction of uric acid and/or impaired renal excretion of uric acid.^{1–3} Uric acid is a product of purine metabolism, which involves xanthine oxidase (XO) in the two final steps (from hypoxanthine to xanthine, then to uric acid). Therefore inhibition of this enzyme has been an obvious target to control uric acid level in blood and eventually to cure gout. In this regard, allopurinol (Fig. 1) has been clinically used to treat hyperuricemia for more than forty years. Recently, febuxostat (Fig. 1) has been introduced. Both of these drugs target xanthine oxidase to inhibit its function. The XO inhibitors block the biosynthesis of uric acid through competitive inhibition, leading to lower uric acid level in blood.^{4,5} Although both of them are inhibitors of XO, their mechanism of action is diverged. The purine analog, allopurinol is a mechanism-based inhibitor of xanthine oxidase.^{5,6} Allopurinol itself is a weak XO inhibitor *in vitro*. However, it is rapidly oxidized by XO *in vivo* to form an active metabolite called oxypurinol, which is a potent XO inhibitor.

On the other hand, febuxostat is a 2-phenylthiazole analog and displays higher inhibitory activity by strong non-competitive binding to active site of XO. However, it has not been proved to be clinically more beneficial compared with allopurinol.^{7–9} Another approach to treat gout is to use recombinant urate oxidase, which directly metabolizes uric acid to allantoin. Pegloticase, approved in 2010, is a pegylated urate oxidase that treats refractory chronic gout.³ Uric acid levels may also be lowered by uricosurics, which increase the urinary excretion of uric acid by interfering the urate absorption from kidney to blood.

Although the link between hyperuricemia and gout has been known for more than hundred years, the intrinsic metabolic relationship between hyperuricemia and diabetes was recently established.^{10,11} Since hyperuricemia becomes serious health problem, it calls for more diverse treatment option. In the recent years, many synthetic scaffolds comprising triazole,¹² isocytosines,^{13,14} pyrimidone¹⁵ and imidazole¹⁶ have been reported to display XO inhibition in the literatures. In this context, we have made an effort to discover novel XO inhibitors based on indolethiazole **6** as shown in Figure 1. The indole rings are frequently utilized as active scaffold in designing target molecules or inhibitors for enzymes and receptors.^{17–19}

Although little was known about the effect of indole scaffold on XO inhibition, it can be found easily in promising anticancer,

* Corresponding authors. Tel.: +82 42 821 5939; fax: +82 42 823 6566 (S.-H.J.); tel.: +82 42 866 2247; fax: +82 42 861 2566 (G.T.K.).

E-mail addresses: jungshh@cnu.ac.kr (S.-H. Jung), gtakim@lgls.com (G.T. Kim).

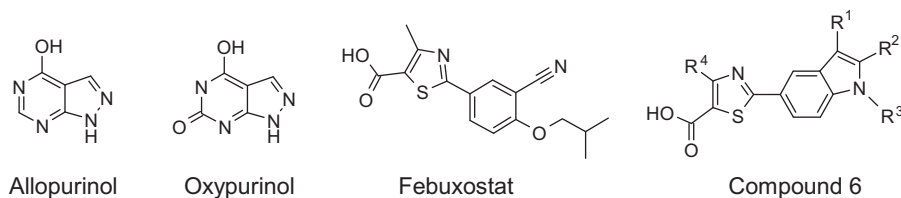


Figure 1. Structures of allopurinol, oxypurinol, febuxostat and compound **6** as xanthine oxidase inhibitors.

antimicrobial, anti-inflammatory, analgesic, anticonvulsants, anti-oxidant and antidiabetic agents,^{17–19} indicating that indole may serve as a prospective scaffold in inhibiting xanthine oxidase.

In order to obtain an agent with better pharmacological profile and in vivo efficacy for the treatment of gout, we incorporated indole moiety into **6** as an isosteric replacement of phenyl moiety of febuxostat as shown in **Figure 1**.

The general synthetic route to **6** is shown in **Scheme 1**. Amide **2** was synthesized from acid **1** using HBTU [2-(1*H*-benzotriazole-1-yl)-1,1,3,3-tetramethyluronium hexafluorophosphate] and ammonium chloride. Amide **2** was converted to thioamides **3** by refluxing with Lawesson's agent in THF. Compound **3** and ethyl 2-chloroacetate were reacted with a catalytic amount of pyridine by refluxing in ethanol to afford indole-5-thiazole **4** in a reasonable yield of 70–85%. Compound **4** was reacted with alkyl bromide and sodium hydride in DMF at room temperature to furnish compound **5**, and this type of reaction allowed the modification of R³ group. Ester **5** was hydrolyzed with sodium hydroxide in aqueous THF and methanol, and the final compound **6** was obtained in a good yield.

The established synthesis led us to evaluate in vitro xanthine oxidase inhibition of **6**. Assay of in vitro XO inhibition activity was performed by measuring the inhibitor concentration needed for 50% inhibition.²⁰ IC₅₀ values of **6e**, **6k**, **6m** and **6n** showed the similar levels to febuxostat. **Tables 1–3** represent the inhibitory activities against XO of the test compound.

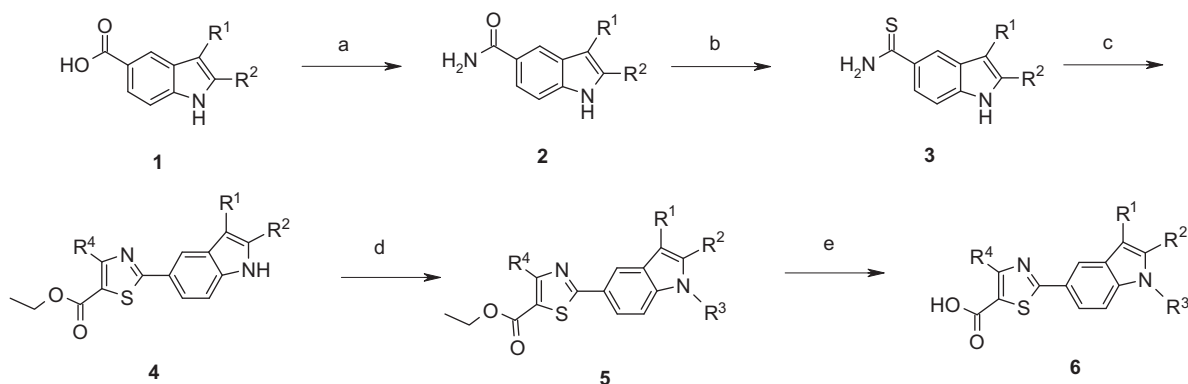
The activities of indole **6a–g** were initially investigated as shown in **Table 1**. Compound **6a** (IC₅₀ = 110 nM) with hydrogen for R¹ and isobutyl group for R³ was found as a hit compound. The previous investigation indicated that an electron-withdrawing group such as nitro, chloro and cyano groups at 2-position in febuxostat plays an important role on xanthine oxidase inhibition.²³ Thus, chloro and nitro groups were introduced at 3-position of **6a**. Chloro compounds **6b**, **6c** and **6d** showed remarkably low IC₅₀ values of 5.7 nM, 7.3 nM and 16.0 nM, respectively. Unfortunately, **6b** and **6d** were not metabolically stable (**Table 1**). Although **6c** exhibited highly potent inhibitory activity (IC₅₀ = 7.3 nM), it

displayed in vivo uric acid-lowering activity of only 18.9%. Compound **6e** with nitro group showed IC₅₀ values of 4.2 nM. However, **6e** was less metabolically stable than **6g** (**Table 1**). Compound **6f** exhibited moderate inhibitory activity. Compound **6g** with cyano group showed an IC₅₀ value of 5.5 nM which was ten times more potent in activity than the original hit compound **6a**. Thus, it was confirmed that substitution with electron-withdrawing group at 3-position of the indole ring increased in vitro XO inhibitory activity.

In order to examine the effect of the substitution at 3-position of the thiazole ring, analogs **6h–k** were prepared and their XO inhibitory activities were tested as shown in **Table 2**. Based on 50% cytotoxic concentration (CC₅₀) using primary rat hepatocytes, **6k** (CC₅₀ = 200 μM) was less cytotoxic than **6g** (CC₅₀ = 82 μM). Therefore, isopropyl group was fixed at 1-position for comparison. Compound **6i** with trifluoromethyl group exhibited high IC₅₀ value of 895.0 nM, and **6j** with methoxy group much increased activity (IC₅₀ = 90.0 nM). Compound **6h** (R⁴ = H) and **6k** (R⁴ = CH₃) displayed better inhibitory activities compared with **6i** and **6j**. Oral exposure in rats with **6h** and **6k** revealed that **6k** exhibited high C_{max} and AUC values as shown in **Table 2**. Therefore, we focused on the modification of **6k** comprising cyano group with various substituents for R² and R³.

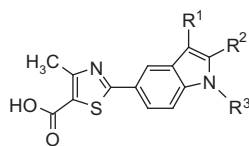
The substitution effect on XO inhibition is summarized in **Table 3**. Most of the compounds in **Table 3** showed good XO inhibitory activity. Further selection was carried out on the basis of in vivo uric acid reduction at 10 mg/kg.

In order to check whether the R² substituent is worthwhile to be varied, **6l** (R² = CH₃) was prepared. It exhibited moderate inhibitory activity (IC₅₀ = 10.7 nM) and low in vivo efficacy. Therefore, our interest was focused on the R³ substituent. Introduction of fluoroisopropyl, hydroxyl isopropyl and methoxy isopropyl group afforded **6m**, **6n** and **6o**, showing potent IC₅₀ values of 4.9 nM, 3.0 nM and 9.0 nM, respectively. Unfortunately, those compounds displayed weak uric acid lowering activity compared to **6k**. Compounds **6p** (R³ = methanesulfonyl ethyl) and **6q** (R³ = acetyl amino ethyl) exhibited moderate inhibitory activities of 9.0 nM and



Scheme 1. Reagents and conditions: (a) HBTU, NH₄Cl, Et₃N, DMF, 74–90%; (b) Lawesson's agent, THF, reflux, 90–95%; (c) ethyl 2-chloroacetate, pyridine, EtOH, reflux, 70–85%; (d) alkyl bromide, sodium hydride, DMF, 70–80%; (e) THF/MeOH = 1:1, 1 N NaOH, 90%.

Table 1
IC₅₀ and metabolic stability of compound **6** with various R¹, R² and R³

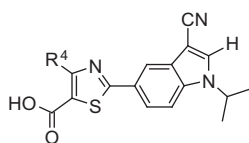


Compound	R ¹	R ²	R ³	In vitro IC ₅₀ (nM)	Metabolic stability ^a (half life, min)
6a	H	H		110	27.5
6b	Cl	H		5.7	6.2
6c	Cl	H		7.3	96.0
6d	Cl	CH ₃		16.0	6.6
6e	NO ₂	H		4.2	79.5
6f	NO ₂	H		12.0	NT ^b
6g	CN	H		5.5	105.7
Febuxostat				3.1–5.5	174.0

^a Metabolic stability was studied in rat liver microsomes (RLM).

^b NT: not tested.

Table 2
The effect of R⁴ in compound **6** on xanthine oxidase inhibition



Compound	R ⁴	In vitro IC ₅₀ (nM)	C _{max} (μg/mL) ^a at 10 mg/kg	AUC _{0–last} (μg h/mL) ^b at 10 mg/kg
6h	H	4.4	0.94	5.39
6i	CF ₃	895.0	NT ^a	NT
6j	OCH ₃	90.0	NT	NT
6k	CH ₃	3.5	3.98	47.31
Febuxostat		3.1–5.5	16.37	61.51

^{a,b} Test compound was administered orally at 10 mg/kg in Sprague-Dawley (SD) rats.

^a NT: not tested.

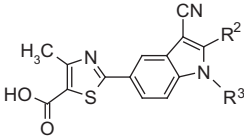
12.3 nM, respectively. Less than 0.02 g/mL of low plasma concentration at 1 h was observed when **6p** or **6q** was orally administered in rats. This result indicates low in vivo efficacy of **6p** or **6q** is caused by low plasma exposure. Compound **6r** with sulfonamide group had good XO inhibitory activity of 6.0 nM, but did not reduce in vivo uric acid level. Thus, hydrophilic substitution for R³ has a harmful effect on in vivo inhibition efficacy. Finally, we decided to install benzyl group for R³ and the hydrophobic effect was investigated. Compounds **6s** and **6t** had good XO inhibitory activities of 3.9 nM and 8.6 nM, but exhibited weak uric acid lowering activities of 10.0% and 16.0% at 10 mg/kg, respectively. Low plasma exposure of **6s** (0.29 g/mL) and **6t** (0.11 g/mL) at 1 h was observed as well when each compound was treated in rats. Their weak in vivo efficacy is attributed to low plasma concentration and low bioavailability in rats.

Among test compounds for XO inhibition, **6k** with cyano group for R¹ was found to display well-balanced and excellent in vitro activity and in vivo efficacy.

To visualize the interaction of indole scaffold with XO enzyme, we performed molecular modeling studies using the Schrodinger Glide program with **6k**. The proposed binding model of **6k** is oriented similarly to febuxostat in its complex with bovine milk XO as shown in Figure 2 (PDB code 1N5X).²⁴ Since the residues around the binding pocket are highly conserved in bovine and human XO, our findings are also applicable to human XO.⁷ The major interactions show the hydrogen bonds among acid group of the inhibitor, Arg880 and Thr1010. Cyano group forms hydrogen bond with Asn768 as well. The thiazole ring that interacts with Glu802 appears to have π–π stacking interaction with Phe914 and Phe1009. Non-bonded interactions are also observed with amino acid residues, Leu648, Phe649, Leu873, Val1011, Phe1013 and Leu1014 in the active site of XO.

The proposed docking model provides us with a reasonable explanation of modification in compounds. In Table 1, substituents of chloro, nitro and cyano groups at R¹ position led to more than 10-fold gain in potency. Based on the docking model, chloro, nitro

Table 3
The effect of R² and R³ in compound **6** on xanthine oxidase inhibition



Compound	R ²	R ³	In vitro IC ₅₀ (nM)	Uric acid inhibition (%) ^a at 1 h, 10 mg/kg
6k	H		3.5	60.0
6l	CH ₃		10.7	8.6
6m	H		4.9	22.3
6n	H		3.0	8.5
6o	H		9.0	14.1
6p	H		12.3	0.0
6q	H		5.6	0.0
6r	H		6.0	0.0
6s	H		3.9	10.0
6t	H		8.6	16.0
Febuxostat			3.1–5.5	

^a Uric acid inhibition was studied in SD rats at 10 mg/kg by oral route.

Table 4
Pharmacokinetic data of **6k** in SD rats^a

Pharmacokinetic parameters	po	iv
Dose (mg/kg)	10	2
C _{max} (μg/mL)	3.98	
AUC _{0–last} (μg h/mL)	47.31	12.39
AUC _{0–infinity} (μg h/mL)	52.87	12.54
T _{max} (h)	6	
T _{1/2} (h)	7.95	4.37
Clearance (mL/h/kg)		161.47
Vd (mL/kg)		634.99
Bioavailability (%)	84.31	

^a n = 3.

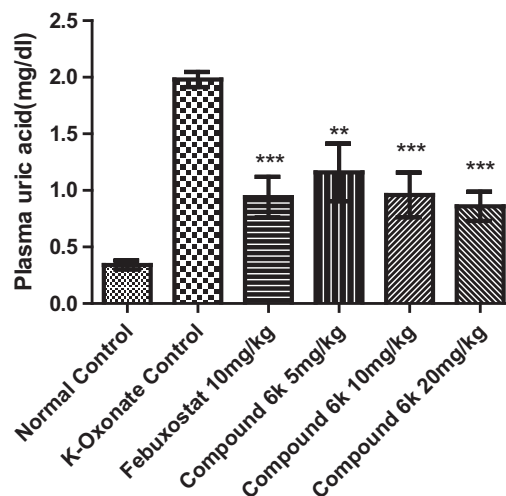


Figure 3. Plasma uric acid concentration (mg/dl) (**P<0.01,***P<0.001: ANOVA and post Dunnet's test).

thiazole acid and appears to loose hydrogen bond between Arg880 and the acid. Thus, compound **6i** shows much less IC₅₀ compared to **6k**.

Pharmacokinetic profile of **6k** was investigated in Sprague-Dawley (SD) rats at a single 10 mg/kg dose by oral route (po) over 24 h. Pharmacokinetic parameters of **6k** were described in Table 4, showing high C_{max} of 3.98 μg/mL, AUC_{0–last} of 47.31 μg h/mL and long half life of 7.95 h. Compound **6k** exhibited excellent oral bioavailability and good in vivo efficacy.

In order to estimate the plasma uric acid-lowering ability, experiments were carried out using oxonic acid-induced high-uric acid model.^{21,22} Figure 3 represents plasma uric acid concentration. The uric acid inhibition rate of **6k** (10 mg/kg) at 1 h after oral administration (putting the plasma uric acid level of normal group as 100% inhibition, and plasma uric acid level of control group as 0% inhibition) was 60%, indicating a suppression rate similar to febuxostat (10 mg/kg). As revealed by the experiment, **6k** exerts an excellent inhibitory effect on XO. Therefore, **6k** can be used as an agent for the treatment and prevention of the diseases associated with human xanthine oxidase such as hyperuricemia and gout.

In summary, we identified a novel indole scaffold for xanthine oxidase inhibition. Among a series of indole derivatives, **6k** exhibited good pharmacokinetic parameters and oral availability. Compound **6k** has excellent plasma uric acid-lowering in vivo efficacy, which will be further developed for clinical studies.

Acknowledgment

We would like to thank Dr. Dongchul Lim for his continuous support to this structure-guided drug discovery project.

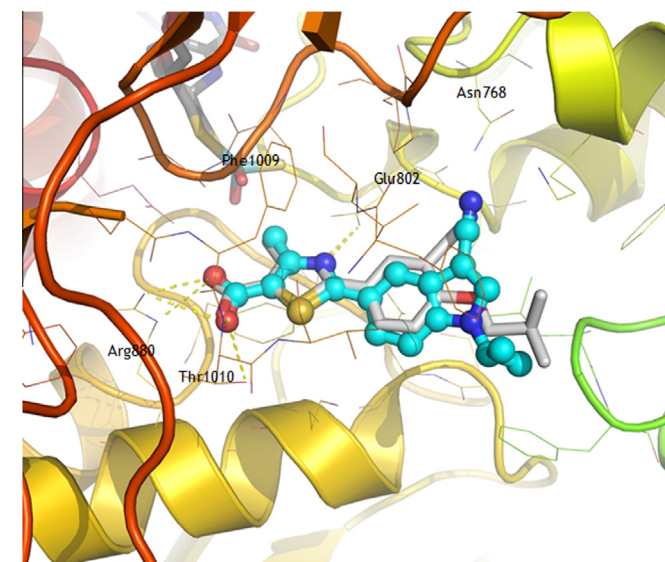


Figure 2. Docking model of bovine XO bound to **6k** (cyan) and febuxostat (gray). The hydrogen bonds are shown in yellow dashed line. Docking results are visualized using PyMol.¹⁹

and cyano groups form hydrogen bonds with Asn768, explaining a significant increase in inhibition for **6b**, **6e** and **6g**. In Table 2, the electronegative substituent such as trifluoromethyl group at R⁴ position lowers electron density of the hydrogen bond acceptor,

References and notes

1. Suresh, E. *Postgrad. Med. J.* **2005**, *81*, 572.
2. Shoji, A.; Yamanaka, H.; Kamatani, N. *Arthritis Rheum.* **2004**, *51*, 321.
3. Adams, J. U. *Nat. Biotech.* **2009**, *27*, 309.
4. Emmerson, B. T. N. *Engl. J. Med.* **1996**, *334*, 445.
5. Okamoto, K.; Eger, B. T.; Nishino, T.; Pai, E. F.; Nishino, T. *Nucleosides Nucleotides Nucleic Acids* **2008**, *27*, 888.
6. Pacher, P.; Nivorozhkin, A.; Szabó, C. *Pharmacol. Rev.* **2006**, *58*, 87.
7. Okamoto, K.; Eger, B. T.; Nishino, T.; Kondo, S.; Pai, E. F.; Nishino, T. *J. Biol. Chem.* **1848**, *2003*, 278.
8. Takano, Y.; Hase-Aoki, K.; Horiuchi, H.; Zhao, L.; Kasahara, Y.; Kondo, S.; Becker, M. A. *Life Sci.* **1835**, *2005*, 76.
9. Ernst, M. E.; Fravel, M. A. *Clin. Ther.* **2009**, *31*, 2503.
10. Johnson, R. J.; Kang, D.-H.; Feig, D.; Kivlighn, S.; Kanellis, J.; Watanabe, S.; Tuttle, K. R.; Rodríguez-Iturbe, B.; Herrera-Acosta, J.; Mazzali, M. *Hypertension* **2003**, *41*, 1183.
11. Li, C.; Hsieh, M.-C.; Chang, S.-J. *Curr. Opin. Rheumatol.* **2013**, *25*, 210.
12. Sato, T.; Ashizawa, N.; Iwanaga, T.; Nakamura, H.; Matsumoto, K.; Inoue, T.; Nagata, O. *Bioorg. Med. Chem. Lett.* **2009**, *19*, 184.
13. Khanna, S.; Burudkar, S.; Bajaj, K.; Shah, P.; Keche, A.; Ghosh, U.; Chandrika, B-Rao.; Sharma, R.; Sivaramkrishnan, H. *Bioorg. Med. Chem. Lett.* **2012**, *22*, 7543.
14. Bajaj, K.; Burudkar, S.; Shah, P.; Keche, A.; Ghosh, U.; Tannu, P.; Khanna, S.; Chandrika, B-Rao.; Sharma, R.; Sivaramkrishnan, H. *Bioorg. Med. Chem. Lett.* **2013**, *23*, 834.
15. Evenas, J.; Edfeldt, F.; Lepisto, M.; Svitacheva, N.; Synnergren, A.; Lundquist, B.; Granse, M.; Tjornebo, A.; Narjes, F. *Bioorg. Med. Chem. Lett.* **2014**, *24*, 1315.
16. Biagi, G.; Costantini, A.; Costantino, L.; Giorgi, I.; Livi, O.; Lundquist, B.; Pecorari, P.; Rinaldi, M.; Scartoni, V. *J. Med. Chem.* **1996**, *39*, 2529.
17. Zhang, M.-Z.; Mulholland, N.; Beattie, D.; Irwin, D.; Gu, Y.-C.; Chen, Q.; Yang, G.-F.; Clough, J. *Eur. J. Med. Chem.* **2013**, *63*, 22.
18. Acton, J. J.; Akiyama, T. E.; Chang, C. H.; Colwell, L.; Debenham, S.; Doebber, T.; Einstein, M.; Liu, K.; McCann, M. E.; Moller, D. E.; Muise, E. S.; Tan, Y.; Thompson, J. R.; Wong, K. K.; Wu, M.; Xu, L.; Meinke, P. T.; Berger, J. P.; Wood, H. B. *J. Med. Chem.* **2009**, *52*, 3846.
19. Hwang, I. K.; Yoo, K. Y.; Li, H.; Park, O. K.; Lee, C. H.; Choi, J. H.; Won, M.-H. *J. Neurosci. Res.* **2009**, *87*, 2126.
20. Assay of xanthine oxidase inhibition activity was performed as follows. Xanthine oxidase originated from butter milk (Sigma) was adjusted to 0.05 U/ml by using 50 mM phosphate buffer, and then added to 96-well plate at 20 μ L/well. 50 mM phosphate buffer was added at 140 μ L/well, and test compounds of various concentrations (10% DMSO phosphate buffer) were added at 20 μ L/well, and pre-incubated for 3 min at room temperature. Immediately after 200 μ M xanthine solution was added at 20 μ L/well, the initial velocity of uric acid formation was determined at 293 nm using microplate reader SpectraMax spectrophotometer. Linear Vmax during 5 min for each test compound concentration was determined as initial velocity. In addition, the initial velocity of the test compound at each concentration was converted to % inhibition rate on the basis of the initial velocity in the absence of the inhibitor, thereby the inhibitor concentration needed for 50% inhibition was calculated as IC₅₀ values. IC₅₀ values of **6e**, **6k**, **6m** and **6n** showed the similar levels to febuxostat. Tables 1–3 represent the inhibitory activities against XO of the test compound.
21. Experiments were carried out using oxonic acid-induced high-uric acid model. Potassium oxonate (300 mg/kg) suspended in 0.8% carboxymethylcellulose solution was intraperitoneally administered to male SD rats of body weight 200 g. One hour after the oxonic acid administration, test compounds dissolved in a solution of poly(ethylene glycol) 400 and ethanol (2:1) were orally administered, and after the time period of 1 h, blood was sampled. Plasma was separated from obtained blood and the uric acid concentration in the plasma was quantified utilizing LC–MS/MS.
22. Osada, Y.; Tsuchimoto, M.; Fukushima, H.; Takahashi, K.; Kondo, S.; Hasegawa, M.; Komoriya, K. *Eur. J. Pharmacol.* **1993**, *241*, 183.
23. Hachioji, S. K.; Hino, H. F.; Hino, M. H.; Hino, M. T.; Hino, I. N.; Hino, Y. O.; Hachioji, K. K.; Hino, H. Y. U.S. Patent 5,614,520, 1997.
24. The docking study of **6k** was performed using the X-ray crystal structure of bovine milk XO (PDB code 1N5X). Flexible docking was carried out using the Schrödinger Glide program with standard precision mode (<http://www.schrodinger.com>). Docking results were visualized using PyMol (<http://www.pymol.org>).